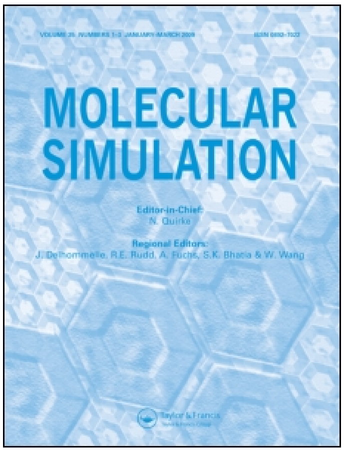

Molecular Simulation
Publication details, including instructions for authors and subscription information:
http://www.informaworld.com/smpp/title~content=t713644482

Reaction Field Simulations of Monatomic and Diatomic Dipolar Fluids

Berthold Saager[a]; Johann Fischer[a]; Martin Neumann[b]
[a] Institut für Thermo-und Fluiddynamik, Ruhr-Universität, Bochum 1, Germany [b] Institut für Experimentalphysik, Universität Wien, Vienna, Austria

To cite this Article Saager, Berthold , Fischer, Johann and Neumann, Martin(1991) 'Reaction Field Simulations of Monatomic and Diatomic Dipolar Fluids', Molecular Simulation, 6: 1, 27 — 49
To link to this Article: DOI: 10.1080/08927029108022138
URL: http://dx.doi.org/10.1080/08927029108022138

Molecular Simulation, 1991, Vol. 6, pp. 27–49
Reprints available directly from the publisher
Photocopying permitted by license only

REACTION FIELD SIMULATIONS OF MONATOMIC AND DIATOMIC DIPOLAR FLUIDS*

BERTHOLD SAAGER and JOHANN FISCHER

Institut für Thermo-und Fluiddynamik, Ruhr-Universität, D-W-4630 Bochum 1, Germany

MARTIN NEUMANN

Institut für Experimentalphysik, Universität Wien, Strudlhofgasse 4, A-1090 Vienna, Austria

(*Received January 1990, accepted April 1990*)

Firstly, the conditions are explored for which molecular dynamics simulations yield reliable thermodynamic results when the reaction field method is applied for dipolar fluids. The influence of the system size, of the scaling method for avoiding the total energy updrift, and of the reaction field dielectric constant are studied. With appropriate conditions, the results for the Stockmayer fluid when compared to previous results show excellent agreement up to very high dipole moments. In the next step the method is applied to two-centre Lennard-Jones plus ideal axial dipole (2CLJD) molecules of elongation $L = 0.505$. For one state point, the influence of the molecular shape as well as of the dipolar strength on energy and pressure is studied in detail. Finally, in the project of developing a physically based equation of state for polar fluids, thermodynamic results are presented for 2CLJD fluids of elongation $L = 0.505$ for four different dipole moments at 29 state points in a temperature and density grid. For these 116 runs which all were performed with vectorized codes on a CYBER 205 also the uncertainties in the results are given as have been estimated from the running averages.

KEY WORDS: Dipolar fluids, Reaction field, Stockmayer fluid, Diatomic dipolar fluid.

1. INTRODUCTION

The interest in simulating dipolar fluids can be either to study dielectric properties, or correlation functions, or thermodynamic properties. One goal in this paper is to arrive at a simple and accurate algorithm for the calculation of thermodynamic properties of nonspherical dipolar molecules taking two-centre Lennard-Jones molecules with ideal dipole along the axis (2CLJD) as a special example. Such simulations are important in several aspects. Firstly, one would like to check theories [1]. Secondly, one may be interested in direct simulations of thermodynamic properties of real fluids. The new refrigerant R152a (CH_3-CHF_2) was recently modelled at 2CLJD fluid and the thermodynamic properties obtained from simulations are in fair agreement with experimental data [2]. Finally, one may think of constructing an equation of state (EOS) with an explicit term for the dipolar contribution to the Helmholtz free energy which is based on simulation results [3].

The problem in simulating dipolar molecules is — as is well known — in the long range of the potential. In principle, there are two possibilities to solve this problem. One method is the lattice simulation (LS) technique [4–11] which makes use of the

---

* Dedicated to Henry V. Kehiaian on the occasion of his 60th birthday.

periodicity of a molecular simulation sample. An alternative is the reaction field (RF) method proposed by Barker and Watts [12], which makes use of the classical Onsager reaction field [13]. Our aim was, presumably in agreement with many practical applicants, to have a simply-to-implement and easy-to-use algorithm. Whilst we do not deny the merits of LS it seems that for our purposes RF is more suitable.

As, however, the RF boundary conditions have not yet been investigated in sufficient detail, the paper starts with exploring the simulation conditions for which a molecular dynamics (MD) code using RF yields sufficiently accurate results for the pressure and the internal energy up to high dipole strengths. For that purpose, we firstly compare with RF and LS literature results for the Stockmayer fluid which seems to be the only simple dipolar fluid for which reliable simulations have been performed. Then, in order to get some deeper understanding, we study explicitely the influence of the system size, of the energy scaling method and of the reaction field dielectric constant on the thermodynamic properties. Having found an appropriate algorithm we apply it to 2CLJD fluids in two respects. Firstly, we explore the effect of molecular shape and present results for molecules of fixed elongation and increasing dipolar strength. Secondly, we wanted to proceed in the construction of an equation of state by performing a variety of runs for 2CLJD fluids. The direct simulation results will also be included in this paper. The correlation techniques for obtaining the dipolar contribution to the Helmholtz free energy as well as applications of the new EOS will be given elsewhere [3].

In the next Section the 2CLJD potential is given as well as formulas for the RF. Details of the MD-algorithm are also summarized there. The results are reported in Section 3. In Subsection 3.1 our Stockmayer results are compared with those of other authors. Then the findings of our studies about different energy scaling methods, RF contributions and system size and about the influence of the RF dielectric constant are reported. Therefrom, we infer the conditions for MD-simulations with RF for 2CLJD liquids, results of which are presented in Section 3.2. Appendix A summarizes some formulas for the ideal dipole and Appendix B gives details about the different energy scaling methods applied.

2. METHODOLOGY

2.1 Intermolecular potential

The system which is under investigation involves 2CLJD interactions. Setting elongation $L = 0$ leads to the Stockmayer potential. The pair potential for the 2CLJD fluid with ideal axial dipole moment is

$$u(r, \omega_i, \omega_j) = u_{2\mathrm{CLJ}}(r, \omega_i, \omega_j) + u_D(r, \omega_i, \omega_j) \tag{1}$$

where r is the separation distance between the centers of mass of the two molecules i and j, and ω_i, ω_j represent the orientations of the molecular axes of the molecules. For the two-center Lennard-Jones (2CLJ) interaction the pair potential is defined by

$$u_{2\mathrm{CLJ}}(r, \omega_i, \omega_j) = \sum_{k=1}^{4} 4\varepsilon \left[\left(\frac{\sigma}{r_k}\right)^{12} - \left(\frac{\sigma}{r_k}\right)^{6}\right) \tag{2}$$

where r_k are the four site-site distances between two rigid diatomic molecules and ε and σ are the Lennard-Jones energy and size parameters. Using customary electrostatic formulas, the interaction between two ideal dipoles $\boldsymbol{\mu}_i$ and $\boldsymbol{\mu}_j$ is described by

$$u_D(r, \omega_i, \omega_j) = -\boldsymbol{\mu}_i \mathbf{T}(\mathbf{r})\, \boldsymbol{\mu}_j \tag{3}$$

The separation distance vector is given by $\mathbf{r} = \mathbf{r}_j - \mathbf{r}_i$ and the **T**-tensor is

$$T_{ab}(r) = \frac{3 r_a r_b}{r^5} - \frac{\delta_{ab}}{r^3} \tag{4}$$

with Kronecker's symbol δ_{ab}.

2.2 Long-range Corrections

In MD simulations we truncate the 2CLJD pair potential at an uniform centre-centre cut-off radius r_c. The truncation effects beyond r_c are corrected by introducing long-range corrections. Then the potential energy u_i of a simple molecule i is approximated by

$$\begin{aligned} u_i = & \sum_{\substack{j \neq i \\ r<r_c}} u_{2\mathrm{CLJ}}(r, \omega_i, \omega_j) + \rho \int_{r>r_c} \langle u_{2\mathrm{CLJ}}(r, \omega_i, \omega_j) \rangle_{\omega_i, \omega_j} \, d\mathbf{r} \\ & - \sum_{\substack{j \neq i \\ r<r_c}} \boldsymbol{\mu}_i \mathbf{T}(\mathbf{r})\, \boldsymbol{\mu}_j - \frac{1}{r_c^3} \cdot \frac{2(\varepsilon_{\mathrm{RF}} - 1)}{2\varepsilon_{\mathrm{RF}} + 1} \cdot \sum_{\substack{j \neq i \\ r<r_c}} \boldsymbol{\mu}_i \cdot \boldsymbol{\mu}_j \\ & - \frac{1}{r_c^3} \cdot \frac{2(\varepsilon_{\mathrm{RF}} - 1)}{2\varepsilon_{\mathrm{RF}} + 1} \cdot \mu^2 . \end{aligned} \tag{5}$$

The second term in Eq. (5) counts for the LJ long-range corrections where $\langle\rangle_{\omega_i, \omega_j}$ represents an angle-averaging over all orientations of a pair of molecules. We assume that the angular pair correlation function $g(r, \omega_i, \omega_j)$ is unity beyond r_c. The angle-average was computed analytically using a formula due to one of us (M.N.). The same equation was later on independently derived by Lustig [14]. The last two terms in equation (5) are the RF-contributions where we separated the electrostatic self-energy from RF in the last term. RF method replaces the dipole–dipole interactions with distances bigger than r_c by an infinite dielectric continuum with dielectric constant $\varepsilon_{\mathrm{RF}}$. This method, combining spherical truncation with classical Onsager reaction field [13], firstly was used by Barker and Watts [12]. Dipolar forces and torques are derived in Appendix A. It comes out that RF does not contribute to the forces but contributes to the torques.

Introducing a tensor $\mathbf{T}_{\mathrm{RF}}$ as

$$T_{\mathrm{RF}_{ab}}(r) = T_{ab}(r) + \frac{1}{r_c^3} \frac{2(\varepsilon_{\mathrm{RF}} - 1)}{2\varepsilon_{\mathrm{RF}} + 1} \delta_{ab} \tag{6}$$

the configurational internal energy per particle is given by

$$\begin{aligned} U = & \frac{1}{N} \left\langle \sum_{\substack{i<j \\ r<r_c}} u_{2\mathrm{CLJ}}(r, \omega_i, \omega_j) \right\rangle_{\mathrm{MD}} + 2\pi\rho \int_{r>r_c} \langle u_{2\mathrm{CLJ}}(r, \omega_i, \omega_j) \rangle_{\omega_i, \omega_j} r^2 dr \\ & - \frac{1}{N} \left\langle \sum_{\substack{i<j \\ r<r_c}} \boldsymbol{\mu}_i \mathbf{T}_{\mathrm{RF}}(\mathbf{r})\, \boldsymbol{\mu}_j \right\rangle_{\mathrm{MD}} - \frac{1}{r_c^3} \cdot \frac{\varepsilon_{\mathrm{RF}} - 1}{2\varepsilon_{\mathrm{RF}} + 1} \cdot \mu^2 \end{aligned} \tag{7}$$

with number of molecules N, volume of the cubic cell V and density $\rho = N/V$. In this equation $\langle\ \rangle_{\mathrm{MD}}$ represents a time-average over an MD run.

For a consistent comparison of RF with LS it is necessary to give some reflections on LS. It was pointed out by de Leeuw *et al.* [6,15] that LS implies a RF too. LS is simulating an infinite large sphere which is constructed by embedding the basic cell with volume V in a space-filling cubic lattice. This infinite sphere is enclosed in a dielectric continuum with $\varepsilon_{\mathrm{RF}}$ thus one may separate the electrostatic self-energy

$$U_{\mathrm{S,LS}} = -\frac{4\pi}{3V}\cdot\frac{\varepsilon_{\mathrm{RF}}-1}{2\varepsilon_{\mathrm{RF}}+1}\cdot\mu^2 \cdot \tag{8}$$

The electrostatic self energy of RF can be separated from equation (7)

$$U_{\mathrm{S,RF}} = -\frac{1}{r_c^3}\cdot\frac{\varepsilon_{\mathrm{RF}}-1}{2\varepsilon_{\mathrm{RF}}+1}\cdot\mu^2 \cdot \tag{9}$$

We set r_c to be half of the box length which yields

$$U_{\mathrm{S,RF}} = \frac{6}{\pi}\,U_{\mathrm{S,LS}} \cdot \tag{10}$$

Thus $U_{\mathrm{S,RF}}$ is approximately two times bigger than $U_{\mathrm{S,LS}}$ for systems of the same size. Calculating pressures of a 2CLJD system, total pressure is given by

$$p = \rho kT + p_{2\mathrm{CLJ}} + p_D \cdot \tag{11}$$

The pressure contribution of the 2CLJ interaction is

$$\begin{aligned} P_{2\mathrm{CLJ}} = &- \frac{\rho}{3N}\left\langle \sum_{\substack{i<j\\ r<r_c}} \mathbf{r}\,\frac{\partial u_{2\mathrm{CLJ}}(r,\omega_i,\omega_j)}{\partial \mathbf{r}} \right\rangle_{\mathrm{MD}} \\ &- \frac{2\pi\rho^2}{3}\int_{r>r_c} \left\langle \mathbf{r}\,\frac{\partial u_{2\mathrm{CLJ}}(r,\omega_i,\omega_j)}{\partial \mathbf{r}} \right\rangle_{\omega_i,\omega_j} r^2\,dr \cdot \end{aligned} \tag{12}$$

Again, the angle-average was computed analytically. Instead using an analog formulation of equation (12) for estimating the dipolar pressure contribution, we use the specific endformula for the virial W_D. For the infinite system one easily can derive

$$W_D = -3\cdot U_D \cdot \tag{13}$$

This yields for the dipolar pressure contribution

$$p_D = -\frac{\rho}{3}\,W_D = \rho\cdot U_D \tag{14}$$

with U_D given by the last two terms of equation (7). The advantage of equation (14) is, that RF is included into pressure, while using $\mathrm{r}(\partial \mathrm{u}/\partial \mathrm{r})$ RF would not contribute. At least, using equation (14), electrostatic self-pressure

$$p_s = \rho\cdot U_S \tag{15}$$

can be calculated. Note that U_D contains U_S and p_D contains p_s.

2.3 MD-algorithm

The MD simulations for the 2CLJD fluid were performed with a program which for its 2CLJ part is based on a computer program due to Haile [16]. The 2CLJ code has been vectorized by one of us (B.S.) for application on a CYBER 205. Into this vectorized version we implemented the additional dipolar contributions using RF geometry. For the 2CLJ part we observed a speedup factor of 10 in comparison to the scalar version running on the same machine. For the 2CLJD system the program executes about 3.5 time steps in 1CPU seconds for 256 molecules and 1 time step in 1CPU seconds for 500 molecules.

The translational equations of motion for the molecular centers of mass are solved by using a fifth order predictor-corrector algorithm due to Gear [17]. For describing the molecular orientations we use quaternion parameters which were introduced in MD by Evans and Murad [18, 19]. The resulting rotational equations of motion are solved by a fourth order predictor-corrector method.

The 2CLJ part of the vectorized program was checked against the original Haile program. Moreover, we compared with a program of Lustig [20] which is based on the method of constrained dynamics due to Ciccotti et al. [21]. The results obtained with both different methods agree within their fluctuations.

We performed simulations for 256 or 500 molecules in a cubic box of constant volume. Periodic boundary conditions and the minimum image criterion were used. The centre-centre cut-off radius was chosen uniformly to be half of the box length.

All runs were started either from an fcc lattice with angular orientations taken from α-nitrogen lattice [22] or from a previous configuration. For production runs up to 10000 time steps we performed 2000 equilibration steps, for longer production runs 10000 equilibration steps were chosen.

To check for the 2CLJD the solution of the rotational equations of motion, we followed an advice due to Adams *et al.* [23]. We froze the translational motion and monitored the total energy over 10000 time steps for a Stockmayer system of 256 molecules in an NVE ensemble (run without any scaling!). The reduced time step $\Delta t^* = \Delta t/(\sigma\sqrt{m/\varepsilon})$ was set to 0.0015 with m being the mass of the whole molecule. For elongated molecules the reduced moment of inertia $I^* = I/(m \cdot \sigma^2)$ can be calculated by $I^* = 0.25 \cdot L^2$ with $L = l/\sigma$. Here l denotes the site-site distance of the two atoms of a diatomic molecule. For small elongations the rotational motion becomes much faster than the translational motion and cannot be described accurately enough.

Table 1 Parameters and reduced units

2CLJ energy parameter	ε
2CLJ size parameter	σ
mass of the molecule	m
site-site distance of the molecule	l
distance	$r^* = r/\sigma$
time	$t^* = t/(\sigma\sqrt{m/\varepsilon})$
elongation	$L = l/\sigma$
moment of inertia	$I^* = I/(m\sigma^2)$
dipole moment	$\mu^* = (\mu^2/(\varepsilon\sigma^3))^{1/2}$
temperature	$T^* = kT/\varepsilon$
density	$\rho^* = \rho\sigma^3$
energy	$u^* = U/\varepsilon$
pressure	$p^* = p\sigma^3/\varepsilon$

Using, that static properties like internal energy and pressure are independent of the value of I^*, we set the moment of inertia arbitrary. For the Stockmayer system with $I^* = 0.025$ we recognized an upward drift in total energy of about 0.02%. If we increased I^* up to 0.064, this corresponds with an elongation $L = 0.505$, the upward drift was reduced to 0.001%. In the following we take for the moment of inertia $0.25 \cdot L^2$, but we ensure that I^* never sinks under 0.025.

It is well known, that for a dipolar system with translational motion an upward drift in total energy appears if RF geometry is used [23]. We study in this paper two different scaling methods. One is a total energy conservation method [24] NVE_x, the other is an isokinetic scaling method NVT_x every x time steps. In the subsection 3.1.2 we give detailed studies about both methods.

3. RESULTS

Working with model fluids it is very convenient to use reduced units which are summarized in Table 1.

3.1 Stockmayer fluid

Setting the elongation $L = 0$ we get the Stockmayer fluid. For this system several results obtained from MD and Monte Carlo (MC) method are available. During our simulations on the Stockmayer fluid we fixed the reduced time step $\Delta t^* = 0.0025$ and the moment of inertia $I^* = 0.025$. All results for energy and pressure include the self-terms. For comparing with previous results it is important to note that we reduce by the 2CLJ energy parameter ε, which is related with the 1CLJ energy parameter by $\varepsilon = \varepsilon_{1CLJ}/4$ for $L = 0$.

3.1.1 Comparison with previous data

For a consistent comparison it is necessary to compare configurational internal energies and pressures with the self-terms included. As these are mostly omitted in previous papers we have added them to the original values if not marked otherwise.

At the beginning we tested our program for a system with $\mu^{*2} = 4$ at a density $\rho^* = 0.8$. In Table 2 we compare with results from Adams *et al.* [23] and Yao *et al.* [25]. The configurational internal energies agree within a deviation smaller than 0.2% and the dipolar contributions show excellent accordance with both authors. The comparison in pressure is not satisfying. While we compare good with Yao *et al.*, our

Table 2 Configurational internal energies and pressures of a Stockmayer fluid with $\mu^{*2} = 4$ at $\rho^* = 0.8$.

T^*	ε_{RF}	u^*	u_D^*	u_S^*	p^*	p_D^*	p_S^*	N	*Prod. steps*	*Type*	*Source*
5.064	7.	−24.68	−3.60	−0.09	6.76	−2.88[a)]	−0.07	108	5860	MD+RF	[23][b)]
5.064	7.	−24.64	−3.60	−0.02	7.18	−2.88	−0.02	500	10000	MD+RF[c)]	†
4.6	∞	−25.18	−3.77	−0.06	4.93	−3.02[a)]	−0.05	108	5000[d)]	MC+LS	[25]
4.6	∞	−25.19	−3.78	−0.03	4.95	−3.02	−0.02	500	10000	MD+RF[c)]	†

a) Calculated in this work via equation (14)

b) We assume that in the original data the self-terms are already included for classical RF

c) NVT_1 method

d) For MC: order of magnitude of (number of moves)/N

† Present results

Table 3 Configurational internal energies and pressures of a highly polar Stockmayer fluid with $\mu^{*2} = 12$ at $T^* = 4.6$ and $\rho^* = 0.822$.

T^*	ε_{RF}	u^*	u_D^*	u_S^*	p^*	p_D^*	p_S^*	N	*Prod. steps*	*Type*	*Source*
4.6	∞	-39.69	–	-0.08	–	–	–	256	$12000^{a)}$	MC + LS	$[26]^{b)}$
4.6	∞	-39.61	-18.88	-0.04	-0.08	$-15.52^{c)}$	-0.03	500	$20000^{a)}$	MC + LS	$[26]^{b)}$
4.62	∞	-39.55	-18.82	-0.04	0.22	$-15.47^{c)}$	-0.03	500	30000	MD + LS	$[26]^{b)}$
4.616	∞	-39.78	-19.08	-0.16	0.12	$-15.68^{c)}$	-0.13	256	50000	MD + RF	[24]
4.596	∞	-39.69	$-18.91^{d)}$	-0.08	-0.25	$-15.54^{d)}$	-0.07	256	100000	MD + LS	[11]
4.600	∞	-39.67	$-18.91^{d)}$	-0.08	-0.20	$-15.54^{d)}$	-0.06	512	150000	MD + RF	[11]
4.6	21	-39.62	-18.86	-0.18	1.89	$-15.50^{c)}$	-0.15	108	15000	MD + LS	[27]
4.6	∞	-39.69	-18.93	-0.15	-0.21	-15.56	-0.13	256	10000	MD + $RF^{e)}$	†
4.6	∞	-39.71	-18.94	-0.15	-0.26	-15.57	-0.13	256	50000	MD + $RF^{e)}$	†
4.6	∞	-39.69	-18.93	-0.08	-0.16	-15.56	-0.07	500	10000	MD + $RF^{e)}$	†

a) For MC: order of magnitude of (number of moves)/N

b) We conclude from [5] that in the original data the self-terms are already included.

c) Calculated in this work via equation (14)

d) This values are not published in the original paper.

e) NVT_1 method

result differs dramatically from the pressure of Adams *et al.* Although it becomes not really clear from [23] if the self-terms are included, the discrepancy in p^* of 0.42 can not be explained.

To have a more stringent test, we performed simulations at a state point first studied in 1981 by Adams *et al.* [26]. At $T^* = 4.6$ and $\rho^* = 0.822$ a Stockmayer system with $\mu^{*2} = 12$ is under investigation. For this highly dipolar system the dielectric constant $\varepsilon_{\mathrm{RF}}$ used in RF or LS usually is set to infinity. In Table 3 we compare with several other authors. As mentioned above the first data are from Adams *et al.* [26]. They performed MD and MC simulations using LS with $\varepsilon_{\mathrm{RF}} = \infty$.

In 1983 Neumann [24] picked up the same system and ran MD simulations with RF. He published further results in 1987 [11], where he used MD with LS following Ladds method [9,10] as well as RF for a bigger system with 512 molecules. In both works $\varepsilon_{\mathrm{RF}}$ is set to infinity.

Petersen *et al.* [27] used LS with $\varepsilon_{\mathrm{RF}} = 21$ in their MD simulations.

We ourself studied this system very intensively and give in Table 3 results from three different runs all using RF. These simulations differ in system size and in simulation length. Our results for the configurational internal energy and the dipolar contributions u_D^* and p_D^* are practically in complete agreement. Only the 2CLJ contribution to the pressure which is about 15 in reduced units and hence the pressure p^* scatters a little bit.

In Figure 1 the comparison in u^*, u_D^* and p^* is illustrated. Our results for u^* and u_D^* are consistent with the previous published ones. Especially the comparison with the newest results of Neumann [11] shows excellent agreement. Larger deviations are observable in pressure. The results from very long production runs [11] and from MC simulations for 500 molecules [26] show negative pressures. This fact is confirmed by all our simulation results. In Figure 1 all simulation results which yield a negative pressure are marked by a window. Looking back to u^* and u_D^* our results show nearly complete agreement with this selected data.

3.1.2 Detailed studies

Using RF for dipolar systems an upward drift in total energy appears [23]. It was our

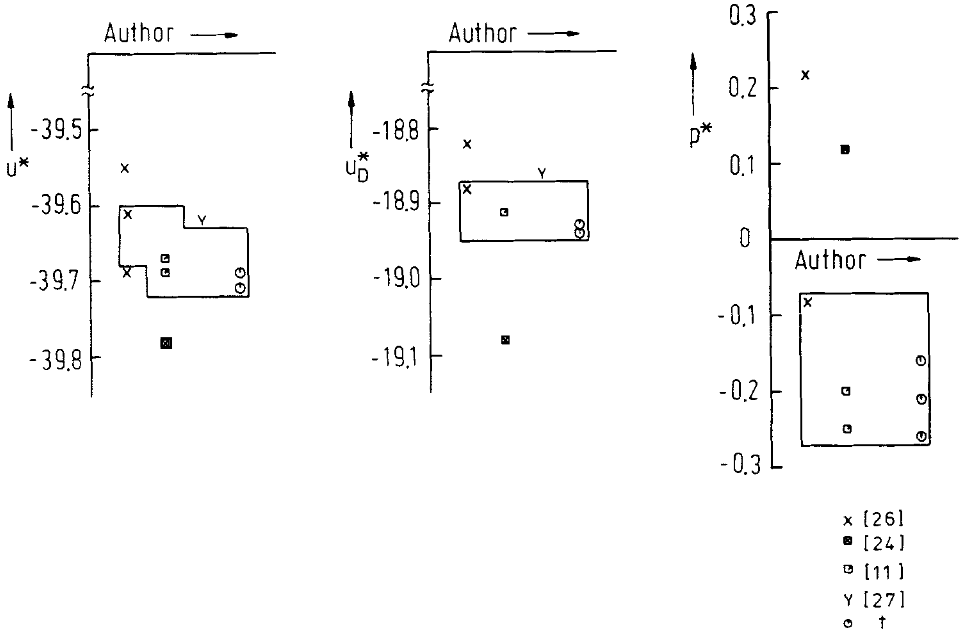

Figure 1 Graphical comparison of results of different authors for configurational internal energies and pressures of a highly polar Stockmayer system (Numerical values are given in Table 3). Results which give a negative pressure are marked by a window.

interest to compare two energy scaling methods. The first is a total energy conservation method [24]. Following this method, total energy is kept constant by rescaling after x time steps the translational and rotational velocities. We did not enforce equipartition between translation and rotation. We call this NVE_x method. In this work we set x equal to 100, so we had an NVE_{100} method. The increase in total energy observed for a Stockmayer fluid at the state point in Table 3 was about 0.75% over 100 time steps for 256 molecules. For 500 molecules the drift is reduced to about 0.33% over 100 time steps.

Alternatively we used a kinetic energy conservation method for the translational and rotational motions for keeping temperature constant. Additionally, we enforce equipartition between translation and rotation. Scaling after every x time steps we call this isokinetic method NVT_x. During our simulations we used NVT_1 and NVT_{100}. In appendix B we give more details about both scaling methods.

In Table 4 we compare NVT_1, NVT_{100} and NVE_{100} at the state point considered in

Table 4 Comparison of different energy scaling methods. Stockmayer system at $T^* = 4.6$ and $\rho^* = 0.822$ with $\mu^{*2} = 12$ and $\varepsilon_{RF} = \infty$; $N = 256$.

T^*	u^*	u_D^*	u_S^*	p^*	p_D^*	p_S^*	*Prod. steps*	*Scaling method*
4.6	−39.69	−18.93	−0.15	−0.21	−15.56	−0.13	10000	NVT1
4.616	−39.72	−18.94	−0.15	−0.25	−15.57	−0.13	10000	NVT100
4.62	−39.70	−18.93	−0.15	−0.23	−15.55	−0.13	9800	NVE100

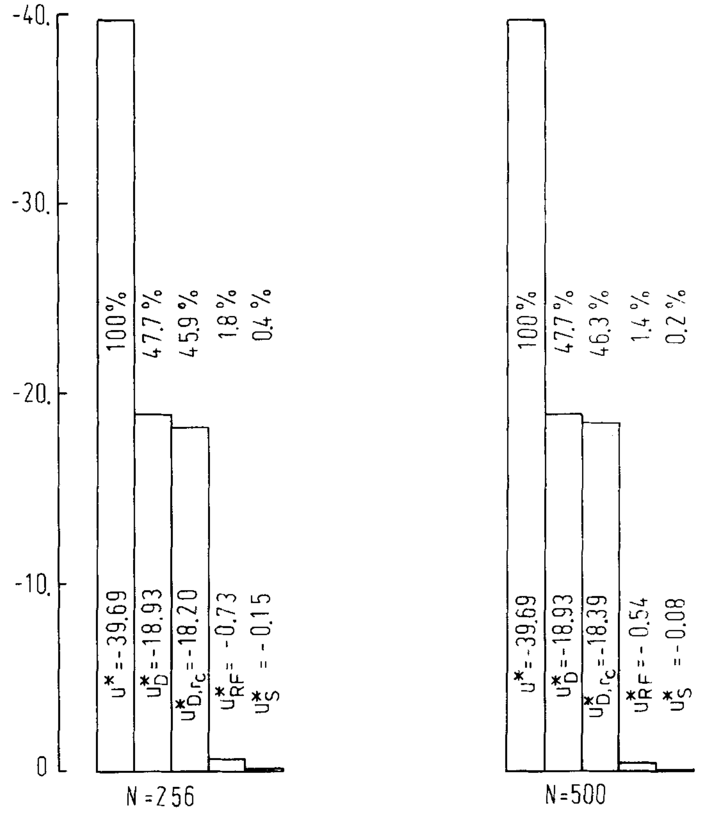

Figure 2 Influence of system size on energy contributions. Stockmayer system at $T^* = 4.6$ and $\rho^* = 0.822$ with $\mu^{*2} = 12$ and $\varepsilon_{\mathrm{RF}} = \infty$. 10000 production steps with NVT$_\mathrm{t}$ method.

Table 3. To our appeasement all three methods led practically to the same results in energy and pressure. One should mention that this consistency is not possible for thermodynamic quantities via fluctuation formulas (second derivatives of the free energy). Hanley and Watts [28] recognized during their MD simulations of methane systematic deviations between c_v from NVE ensemble and isokinetic NVT ensemble. They used the fluctuation formulas of Lebowitz *et al.* [29] for the microcanonical ensemble. Using the same formulas Torro-Labbé *et al.* [30] found out that only NVE yields correct specific heats, whereas isokinetic NVT leads to systematically wrong results in c_v.

We also investigated the system size dependence of the RF method. To distinguish the RF contributions we define

$$u_{D,r_c}^* = -\frac{1}{N}\left\langle \sum_{\substack{i<j\\ r<r_c}} \mu_i^* \mathbf{T}^*(\mathbf{r}^*)\mu_j^* \right\rangle_{\mathrm{MD}} \qquad (16)$$

and

Table 5 Influence of dielectric constant ε_{RF}. Stockmayer system at $T^* = 4.6$ and $\rho^* = 0.822$ with $\mu^{*2} = 12$. $N = 500$, 10000 prod. steps, NVT$_1$ method.

ε_{RF}	u^*	u^*_{2CLJ}	u^*_D	u^*_S	p^*	p^*_{2CLJ}	p^*_D	p^*_S
1.	−39.99	−20.80	−19.19	0.	−0.55	15.22	−15.77	0.
2.	−39.73	−20.76	−18.97	−0.03	−0.18	15.42	−15.60	−0.03
5.	−39.63	−20.75	−18.88	−0.06	−0.11	15.41	−15.52	−0.05
10.	−39.62	−20.76	−18.86	−0.07	−0.17	15.33	−15.50	−0.06
50.	−39.67	−20.77	−18.90	−0.08	−0.20	15.34	−15.54	−0.06
100.	−39.65	−20.76	−18.89	−0.08	−0.16	15.37	−15.53	−0.06
∞	−39.69	−20.76	−18.93	−0.08	−0.16	15.40	−15.56	−0.07

$$u^*_{\mathrm{RF}} = -\frac{1}{N}\cdot\frac{1}{r_c^{*3}}\cdot\frac{2(\varepsilon_{\mathrm{RF}}-1)}{2\varepsilon_{\mathrm{RF}}+1}\left\langle \sum_{\substack{i<j\\ r<r_c}} \boldsymbol{\mu}^*_i\cdot\boldsymbol{\mu}^*_j \right\rangle_{\mathrm{MD}} + u^*_S \qquad (17)$$

with

$$u^*_D = u^*_{D,r_c} + u^*_{\mathrm{RF}} \cdot \qquad (18)$$

Comparing equations (16,17) with equation (7) the $\mathrm{T_{RF}}$-tensor is decomposed to collect all RF contributions in one term u^*_{RF}. Here u^*_{D,r_c} gives the dipolar energy only from dipole–dipole interactions within the cut-off sphere. We compare the two simulation runs over 10000 production steps from Table 3 with 256 and 500 molecules, respectively. A graphical representation of the different energy contributions is given in Figure 2. Increasing system size increases the cut-off sphere and thus decreases the RF contribution to energy as expected.

To estimate the effective influence of RF on the results, we performed simulations with and without RF. In addition we studied the influence of the dielectric constant

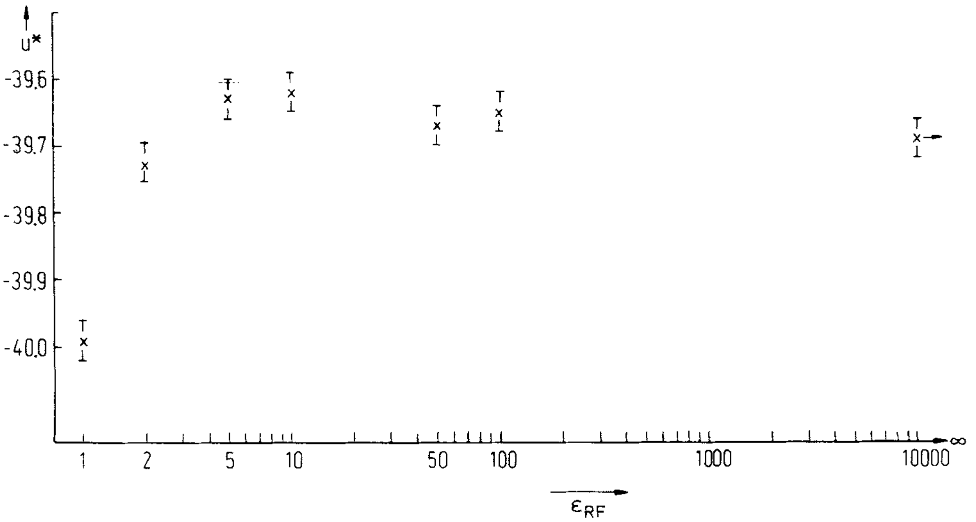

Figure 3 Influence of $\varepsilon_{\mathrm{RF}}$ on u^*. Stockmayer system at $T^* = 4.6$ and $\rho^* = 0.822$ with $\mu^{*2} = 12$.

by variing ε_{RF} from unity to infinity. All simulations were performed for 500 molecules over 10000 production steps. Again the state point was taken from Table 3 and the dipole strength was fixed to $\mu^{*2} = 12$. The results are presented in Table 5 and in Figure 3 we plotted u^* over ε_{RF}. Since the 2CLJ contribution u^*_{2CLJ} is nearly constant, the behaviour of u^* and u^*_D over ε_{RF} is very close. We learn from Figure 3 that for $\varepsilon_{RF} \geqslant 5$ the results are already independent from ε_{RF}. Neumann [11] calculated with $\varepsilon_{RF} = \infty$ a bulk dielectric constant $\varepsilon \approx 65$. Setting $\varepsilon_{RF} = \varepsilon$ or $\varepsilon_{RF} = \infty$ does not affect the results. We conclude that we will set $\varepsilon_{RF} = \infty$, if we have no knowledge about the bulk dielectric constant. A further very important conclusion from Figure 3 is that switching RF off ($\varepsilon_{RF} = 1$) leads intrinsically to wrong results. This is illustrated by comparing for the 500 molecules system u^* for $\varepsilon_{RF} = 1$ and u^* for $\varepsilon_{RF} = \infty$. The effective influence of RF is given by

$$u^*_{RF,eff} = u^*(\varepsilon_{RF}) - u^*(\varepsilon_{RF} = 1). \tag{19}$$

Setting $\varepsilon_{RF} = \infty$ we get $u^*_{RF,eff} = 0.30$. This value can be compared with $u^*_{RF} = -0.54$ (equation (17)) which we take from Figure 2 (500 molecules). The conclusion is that a simulation run neglecting dipolar long-range interactions samples over a different trajectory in phase space than a simulation run using RF or LS.

3.3 Elongated molecules

During our literature investigations we found only a work of de Leeuw and Quirke [31] simulating a 2CLJD system. They give results for the configurational internal energy for 4 different elongations $L > 0$ calculated from MC simulations. We checked the fluid conditions of their state points using 2CLJ phase equilibria data [32–34] and found that all state points appear to be in the two-phase region. Adding a dipole to 2CLJ decreases the critical temperature and shifts the bubble line up [1]. Thus switching a dipole on strengthens the effect. Nevertheless, we tried MD simulations because the authors found that no phase separation occured during their simulations. We set the time step $\Delta t^* = 0.0015$ and performed after an equilibration of 2000 steps 10000 production steps for 500 molecules. At all four state points in our simulations configurational internal energy and pressure drifted away. At some state points the drift started directly at the beginning, other runs seemed to be stable up to about 5000 time steps but then drifted away also. For that reason we can not compare our simulations with previous 2CLJD results.

For 2CLJD a typical simulation run consists of 2000 equilibration steps and 10000 time steps for production. The RF dielectric constant is set to $\varepsilon_{RF} = \infty$. A first study was made to see the effect of the molecular shape. Following Bohn *et al.* [35] we work with corresponding state points which are defined as having the same reduced temperature $\tilde{T}$ and density $\tilde{\rho}$ with respect to the pseudocritical quantities T_p and ρ_p of the nonpolar liquid which were reported earlier [32].

$$\tilde{T} = T/T_p = T^*/T^*_p \tag{20}$$

$$\tilde{\rho} = \rho/\rho_p = \rho^*/\rho^*_p \cdot \tag{21}$$

With the same scaling quantities we define thermodynamically reduced dipole moments $\tilde{\mu}$, energies $\tilde{u}$ and pressures $\tilde{p}$ as

$$\tilde{\mu}^2 = \frac{\mu^2 \cdot \rho_p}{k \cdot T_p} = \mu^{*2} \cdot \rho^*_p / T^*_p \tag{22}$$

Table 6 Simulation results for L = 0 and L = 0.505 at corresponding conditions $\tilde{T} = 0.79$, $\tilde{\rho} = 2.63$ and $\tilde{\mu}^2 = 2.14$.

L	T^*	ρ^*	μ^{*2}	u^*	u_D^*	p^*	p_D^*
0.	4.6	0.822	12	−39.69	−18.93	−0.16	−15.56
0.505	2.43	0.533	9.77	−19.66	− 7.30	1.14	− 3.89

$$\tilde{u} = \frac{U}{kT_p} = u^*/T_p^* \tag{23}$$

$$\tilde{p} = \frac{p}{\rho_p \cdot k \cdot T_p} = p^*/(\rho_p^* \cdot T_p^*). \tag{24}$$

Starting from the state point in Table 3 a simulation run was performed for $L = 0.505$ at corresponding conditions at the same $\tilde{T}$, $\tilde{p}$ and $\tilde{\mu}$. The results in the usual reduced units are compared in Table 6. To study the effect of molecular shape at corresponding conditions one has to compare the thermodynamically reduced properties $\tilde{u}$ and $\tilde{p}$. This comparison together with the pseudocritical quantities T_p^* and ρ_p^* is given in Table 7. From this table we learn that the effect of the elongation is not as big as one may conclude from Table 6. Nevertheless, the influence of the dipole decreases for $L = 0.505$. For elongations $L > 0$ the angular orientations of the molecules are mutual influenced by 2CLJ on the one side and by dipolar interactions on the other side.

As already indicated a major reason for our algorithm development was the aim to construct a physically based equation of state. Hence, having a reliable algorithm, the next step was to perform for one fixed elongation ($L = 0.505$) simulations with different dipole moments at state points in a temperature and density grid. The direct simulation results will also be presented here, whilst the correlation for obtaining the dipolar contribution to the Helmholtz free energy will be presented elsewhere [3].

As a first orientation we run simulations at $T^* = 3.078$ and $\rho^* = 0.466$ variing the dipole moment $\mu^{*2} = 0, 2, 4, 6, 8, 10$ and 12. The results are collected in Table 8. In the table results from additional runs are included which show their reproducibility. In Figure 4 we illustrate the influence of the dipole moment on energy and pressure. We learn from the figure that for describing energy and pressure as function of the dipole strength it is not necessary to have so many points of support at high dipole moments.

To cover the whole fluid region we constructed a lattice of 29 state points in the T,ρ-plane. Table 9 gives an overview how the state points are distributed. For the following MD simulations we restricted to the dipole moments $\mu^{*2} = 2, 4, 8$ and 12. Thus we performed 116 runs. Calculating thermodynamic properties from simulations the problem of estimating the statistical uncertainties arises. We made for each run a plot of the running average of the internal energy u^*, the dipolar contribution

Table 7 Effect of molecular shape at corresponding conditions.

L	T_p^* [32]	ρ_p^* [32]	$\tilde{T}$	$\tilde{\rho}$	$\tilde{\mu}^2$	$\tilde{u}$	$\tilde{u}_D$	$\tilde{p}$	$\tilde{p}_D$
0.	5.832	0.3128	0.79	2.63	2.14	−6.81	−3.25	−0.09	−8.53
0.505	3.078	0.2028	0.79	2.63	2.14	−6.39	−2.37	1.83	−6.23

Table 8 2CLJD with $L = 0.505$ at $T^* = 3.078$ and $\rho^* = 0.466$ with $\varepsilon_{RF} = \infty$. *If* $\mu^{*2} = 0$, *256 molecules*, else 500 molecules.

μ^{*2}	u^*	u_D^*	u_s^*	p^*	p_D^*	p_s^*
0.	−10.82	0.	0.	2.61	0.	0.
2.	−11.31	−0.53	−0.01	2.46	−0.25	−0.005
	−11.32	−0.52	−0.01	2.47	−0.24	−0.005
4.	−12.38	−1.63	−0.01	2.16	−0.76	−0.005
	−12.37	−1.63	−0.01	2.18	−0.76	−0.005
6.	−13.73	−3.06	−0.02	1.80	−1.43	−0.01
8.	−15.24	−4.66	−0.03	1.40	−2.17	−0.01
	−15.22	−4.66	−0.03	1.44	−2.17	−0.01
10.	−16.90	−6.42	−0.04	1.00	−3.00	−0.02
12.	−18.65	−8.30	−0.04	0.63	−3.87	−0.02
	−18.64	−8.29	−0.04	0.63	−3.87	−0.02
	−18.64	−8.29	−0.04	0.63	−3.87	−0.02

u_D^* and the total pressure p^*. Therefrom we estimated the statistical uncertainties Δu^*, Δu_D^* and Δp^*. All results together with the uncertainties are given in Table 10. At same state points reproduction runs were performed which are marked in the table. On the gas side at presumably metastable state points drifts in internal energy were observed.

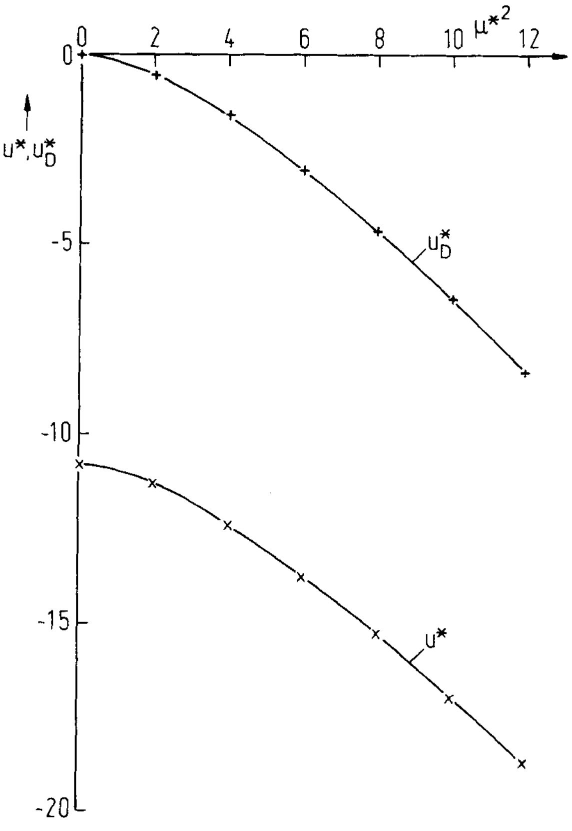

Figure 4a Energies u^* and u_D^* for 2CLJD with $L = 0.505$ at $T^* = 3.078$ and $\rho^* = 0.466$ with $\varepsilon_{RF} = \infty$.

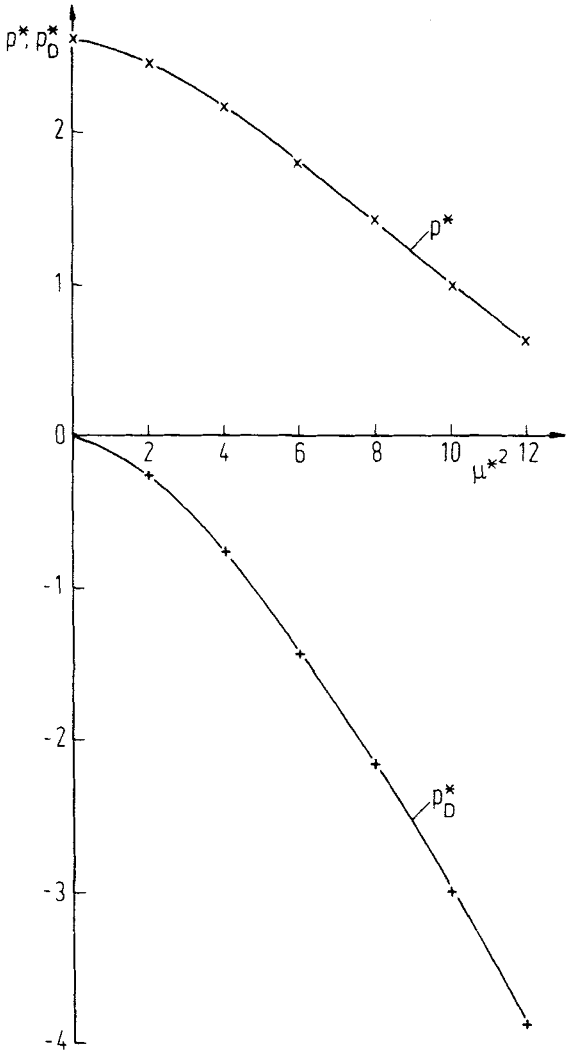

Figure 4b Pressures p^* and p_D^* for 2CLJD with $L = 0.505$ at $T^* = 3.078$ and $\rho^* = 0.466$ with $\varepsilon_{RF} = \infty$.

Table 9 The distribution of the 29 state points in the T, ρ-plane for which MD-simulations were performed with four different dipole moments (500 molecules; $L = 0.505$).

ρ/ρ_p T/T_p	*0.3*	*0.7*	*1.0*	*1.5*	*1.9*	*2.3*	*2.7*	*3.1*
2.0	X	X	X	X	X	X	X	X
1.5	X	X	X	X	X	X	X	X
1.0	X	X	X	X	X	X	X	X
0.7						X	X	X
0.5							X	X

Table 10 Internal energies, dipolar energy contributions and pressures as well as their uncertainties for 116 systems of 2CLJD molecules of elongation $L = 0.505$. All runs were performed for 500 particles and over 10000 time steps. Reproduction runs are marked by *R*.

Run	ρ^*	T^*	μ^{*2}	u^*	u_D^*	p^*	Δu^*	Δu_D^*	Δp^*
1	.06084	3.0780	2.	−1.686	−.086	.142	.060	.010	.0025
2	.06084	3.0780	4.	−2.063	−.355	.135	.050	.015	.0025
2*R*				−2.044	−.351	.136	.050	.015	.0025
3	.06084	3.0780	8.	−3.300	−1.393	.110	.100	.050	.0025
3*R*				−3.299	−1.395	.109	.100	.050	.0025
4$^{a)}$	.06084	3.0780	12.	−5.544	−3.299	.074	.300	.150	.0025
4*R*$^{a)}$				−5.272	−3.108	.075	.300	.150	.0025
5	.06084	4.6170	2.	−1.443	−.060	.259	.035	.005	.002
6	.06084	4.6170	4.	−1.570	−.210	.256	.035	.010	.002
7	.06084	4.6170	8.	−2.232	−.822	.239	.035	.030	.002
8	.06084	4.6170	12.	−3.415	−1.899	.211	.035	.030	.002
9	.06084	6.1560	2.	−1.299	−.041	.373	.035	.010	.003
10	.06084	6.1560	4.	−1.407	−.157	.371	.035	.010	.003
11	.06084	6.1560	8.	−1.887	−.626	.357	.035	.020	.003
12	.06084	6.1560	12.	−2.655	−1.377	.335	.035	.035	.003
13	.14200	3.0780	2.	−3.744	−.188	.235	.050	.010	008
14	.14200	3.0780	4.	−4.616	−.725	.202	.100	.015	.008
15$^{a)}$	.14200	3.0780	8.	−6.438	−2.412	.119	.100	.035	.008
15*R*$^{a)}$				−6.368	−2.401	.115	.100	.035	.008
16$^{a)}$	.14200	3.0780	12.	−10.924	−5.528	.020	-	-	.015
16*R*$^{a)}$				−9.858	−5.134	.014	-	-	.015
17	.14200	4.6170	2.	−3.230	−.122	.591	.035	.010	.007
18	.14200	4.6170	4.	−3.591	−.472	.563	.035	.015	.007
19	.14200	4.6170	8.	−4.797	−1.633	.486	.035	.030	.007
20	.14200	4.6170	12.	−6.629	−3.404	.395	.035	.040	.007
21	.14200	6.1560	2.	−2.991	−.088	.911	.050	.010	.010
22	.14200	6.1560	4.	−3.263	−.360	.904	.050	.015	.010
23	.14200	6.1560	8.	−4.178	−1.302	.834	.050	.025	.010
24	.14200	6.1560	12.	−5.593	−2.696	.762	.050	.040	.010
25	.20280	3.0780	2.	−5.234	−.255	.268	.080	.010	.015
26	.20280	3.0780	4.	−5.935	−.882	.216	.080	.015	.015
27$^{b)}$	.20280	3.0780	8.	−8.477	−2.991	.092	.080	.030	.015
28$^{a)}$	.20280	3.0780	12.	−12.580	−6.186	−.031	.500	.200	.015
28*R*$^{a)}$				−12.031	−6.018	−.041	.500	.200	.015
29$^{c)}$	.20280	4.6170	2.	−4.569	−.170	.870	.025	.010	.015
30	.20280	4.6170	4.	−5.014	−.626	.817	.025	.010	.015
31	.20280	4.6170	8.	−6.557	−2.147	.694	.025	.020	.015
32	.20280	4.6170	12.	−8.646	−4.237	.519	.050	.050	.015
32*R*				−8.613	−4.226	.523	.050	.050	.015
33	.20280	6.1560	2.	−4.208	−.129	1.428	.040	.010	.020
34	.20280	6.1560	4.	−4.588	−.495	1.406	.040	.010	.020
35	.20280	6.1560	8.	−5.818	−1.742	1.302	.040	.015	.020
36	.20280	6.1560	12.	−7.513	−3.509	1.124	.040	.025	.020
37	.30420	3.0780	2.	−7.462	−.350	.398	.065	.100	.030
38	.30420	3.0780	4.	−8.289	−1.167	.303	.065	.015	.030
39	.30420	3.0780	8.	−10.638	−3.559	.001	.065	.025	.030
40$^{b)}$	.30420	3.0780	12.	−14.000	−6.724	−.256	.065	.050	.030
40*R*$^{b)}$				−13.931	−6.705	−.218	.065	.050	.030
41	.30420	4.6170	2.	−6.814	−.253	1.668	.025	.010	.025
42	.30420	4.6170	4.	−7.445	−.900	1.585	.025	.015	.025
43	.30420	4.6170	8.	−9.307	−2.851	1.278	.025	.035	.025
44	.30420	4.6170	12.	−11.801	−5.423	.942	.025	.035	.025
45	.30420	6.1560	2.	−6.361	−.210	2.871	.040	.010	.030
46	.30420	6.1560	4.	−6.828	−.724	2.781	.040	.015	.030

Table 10 (continued.)

Run	ρ^*	T^*	μ^{*2}	u^*	u_D^*	p^*	Δu^*	Δu_D^*	Δp^*
47	.30420	6.1560	8.	−8.448	−2.404	2.551	.040	.025	.030
48	.30420	6.1560	12.	−10.640	−4.701	2.216	.040	.030	.030
49	.38532	3.0780	2.	−9.392	−.442	.871	.020	.010	.025
50	.38532	3.0780	4.	−10.302	−1.390	.684	.020	.010	.025
51	.38532	3.0780	8.	−12.919	−4.106	.259	.020	.015	.025
52[b)]	.38532	3.0780	12.	−16.055	−7.409	−.299	.045	.030	.025
52*R*[b)]				−16.120	−7.440	−.282	.045	.030	.025
53	.38532	4.6170	2.	−8.580	−.316	3.029	.020	.010	.030
54	.38532	4.6170	4.	−9.353	−1.106	2.873	.020	.020	.030
55	.38532	4.6170	8.	−11.554	−3.421	2.471	.020	.025	.030
56	.38532	4.6170	12.	−14.292	−6.336	1.897	.020	.030	.030
57	.38532	6.1560	2.	−7.942	−.260	5.091	.035	.015	.040
58	.38532	6.1560	4.	−8.600	−.938	4.905	.035	.020	.040
59	.38532	6.1560	8.	−10.493	−2.957	4.526	.035	.050	.040
60	.38532	6.1560	12.	−13.005	−5.592	3.954	.035	.050	.040
61	.46644	2.1546	2.	−12.088	−.658	.129	.025	.010	.045
62	.46644	2.1546	4.	−13.310	−1.933	−.215	.025	.020	.045
63	.46644	2.1546	8.	−16.436	−5.253	−.972	.025	.030	.045
64	.46644	2.1546	12.	−20.126	−9.158	−1.744	.025	.035	.045
65	.46644	3.0780	2.	−11.315	−.524	2.469	.025	.010	.035
66	.46644	3.0780	4.	−12.371	−1.634	2.176	.025	.020	.035
67	.46644	3.0780	8.	−15.218	−4.657	1.445	.025	.025	.035
68	.46644	3.0780	12.	−18.638	−8.292	.631	.025	.050	.035
69	.46644	4.6170	2.	−10.256	−.398	6.023	.020	.005	.040
70	.46644	4.6170	4.	−11.147	−1.318	5.701	.020	.015	.040
71	.46644	4.6170	8.	−13.624	−3.958	5.058	.020	.015	.040
72	.46644	4.6170	12.	−16.717	−7.236	4.204	.020	.025	.040
73	.46644	6.1560	2.	−9.356	−.337	9.231	.020	.010	.050
74	.46644	6.1560	4.	−10.096	−1.124	9.031	.020	.015	.050
75	.46644	6.1560	8.	−12.306	−3.463	8.418	.020	.025	.050
76	.46644	6.1560	12.	−15.176	−6.488	7.532	.020	.035	.050
77	.54756	1.5390	2.	−14.895	−.900	−.165	.020	.010	.045
78	.54756	1.5390	4.	−16.389	−2.475	−.669	.020	.015	.045
79	.54756	1.5390	8.	−20.049	−6.372	−1.794	.020	.015	.045
80	.54756	1.5390	12.	−24.161	−10.787	−2.904	.020	.020	.045
81	.54756	2.1546	2.	−14.075	−.762	2.704	.025	.015	.040
82	.54756	2.1546	4.	−15.452	−2.209	2.204	.025	.025	.040
83	.54756	2.1546	8.	−18.880	−5.857	1.095	.025	.025	.040
84	.54756	2.1546	12.	−22.803	−10.068	−.050	.025	.025	.040
85	.54756	3.0780	2.	−13.033	−.623	6.444	.025	.010	.050
86	.54756	3.0780	4.	−14.252	−1.895	5.977	.025	.015	.050
87	.54756	3.0780	8.	−17.392	−5.247	4.990	.025	.025	.050
88	.54756	3.0780	12.	−21.144	−9.244	3.751	.025	.025	.050
88*R*				−21.158	−9.272	3.770	.025	.025	.050
89	.54756	4.6170	2.	−11.545	−.476	11.970	.020	.010	.050
90	.54756	4.6170	4.	−12.577	−1.563	11.564	.020	.010	.050
91	.54756	4.6170	8.	−15.392	−4.549	10.593	.020	.015	.050
92	.54756	4.6170	12.	−18.807	−8.189	9.475	.020	.025	.050
93	.54756	6.1560	2.	−10.240	−.387	16.898	.025	.015	.075
94	.54756	6.1560	4.	−11.139	−1.324	16.559	.025	.020	.075
95	.54756	6.1560	8.	−13.685	−4.019	15.634	.025	.020	.075
96	.54756	6.1560	12.	−16.853	−7.402	14.589	.025	.025	.075
97	.62868	1.5390	2.	−16.686	−1.043	5.054	.025	.010	.060
98	.62868	1.5390	4.	−18.325	−2.786	4.420	.025	.020	.060
99	.62868	1.5390	8.	−22.326	−7.032	2.775	.025	.020	.060
100	.62868	1.5390	12.	−26.725	−11.756	1.122	.025	.030	.060

Table 10 (continued.)

Run	ρ^*	T^*	μ^{*2}	u^*	u_D^*	p^*	Δu^*	Δu_D^*	Δp^*
101	.62868	2.1546	2.	−15.527	− .889	9.486	.025	.015	.075
102	.62868	2.1546	4.	−17.086	− 2.502	8.716	.025	.020	.075
103	.62868	2.1546	8.	−20.850	− 6.506	7.211	.025	.020	.075
104	.62868	2.1546	12.	−25.126	−11.072	5.505	.025	.025	.075
105	.62868	3.0780	2.	−14.070	− .731	15.148	.025	.015	.060
106	.62868	3.0780	4.	−15.432	− 2.158	14.540	.025	.020	.060
107	.62868	3.0780	8.	−18.953	− 5.893	13.070	.025	.025	.060
108	.62868	3.0780	12.	−23.039	−10.244	11.410	.025	.030	.060
109	.62868	4.6170	2.	−11.992	− .568	23.376	.030	.015	.070
110	.62868	4.6170	4.	−13.186	− 1.788	22.730	.030	.015	.070
111	.62868	4.6170	8.	−16.375	− 5.139	21.331	.030	.020	.070
112	.62868	4.6170	12.	−20.124	− 9.139	19.816	.030	.025	.070
113	.62868	6.1560	2.	−10.249	− .475	30.474	.040	.025	.085
114	.62868	6.1560	4.	−11.251	− 1.531	30.027	.040	.025	.085
115	.62868	6.1560	8.	−14.139	− 4.585	28.780	.040	.050	.085
116	.62868	6.1560	12.	−17.660	− 8.341	27.374	.040	.050	.060
116*R*				−17.670	− 8.355	27.388	.040	.050	.060

[a] Drift (presumably metastable)
[b] Mechanically unstable
[c] 8500 time steps

The results of these runs are only given for illustration and completeness and are marked in Table 10 as well. At medium densities some runs could be performed in mechanically unstable regions without drifting away within the duration of 10000 time steps. Again we marked these runs in the table. The dipolar pressure contributions p_D^* and Δp_D^* can be calculated by equation (14). To complete our investigations, examples for the running averages of u^*, u_D^* and p^* are shown in Figures 5 and 6 for two state points, one in the gas and another in the liquid.

4. SUMMARY AND CONCLUSION

We fixed the conditions and parameters for simulating 2CLJD fluids by setting the elongation $L = 0$ to make comparison with the Stockmayer system. Our Stockmayer results show excellent agreement with the best previously published results. Our results confirm what was found by Neumann *et al.* [36] and Adams *et al.* [26] before, that for computing thermodynamic properties the easy to implement RF method yields as good results as the more complicated LS techniques. Two different energy scaling methods were investigated, both yield the same results in energy and pressure. We pointed out that neglecting dipolar long-range interactions gives a principle wrong trajectory. Variation of the RF dielectric constant ε_{RF} teaches us that for bigger systems the simulation results are independent from the exact bulk dielectric constant.

In the second part we performed simulations for dipolar molecules of elongation $L = 0.505$. The influence of elongation was illustrated at a state point corresponding to a previously considered Stockmayer system. Then a large number of results were presented in a temperature, density and dipole moment grid which are the basis for a physically founded equation of state for dipolar fluids.

Acknowledgement

Teile dieser Arbeit wurden von der Deutschen Forschungsgemeinschaft im Schwer-

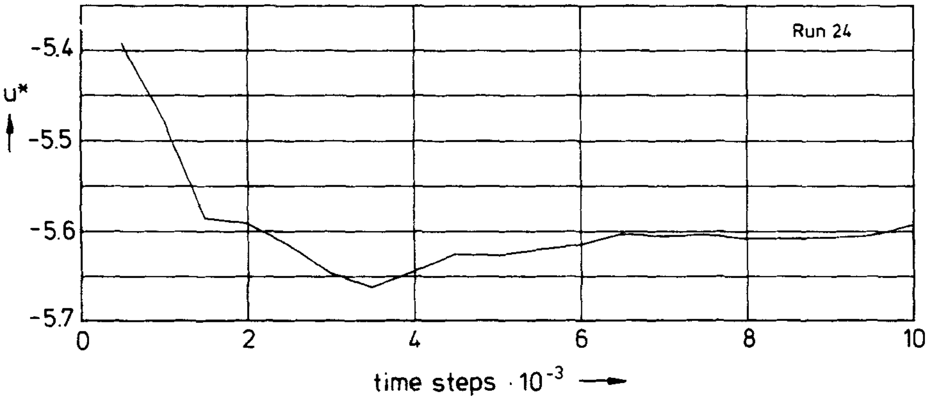

Figure 5a Running average of the configurational internal energy at $\rho^* = 0.142$, $T^* = 6.156$ and $\mu^{*2} = 12$ (run 24). This is an example for the gas.

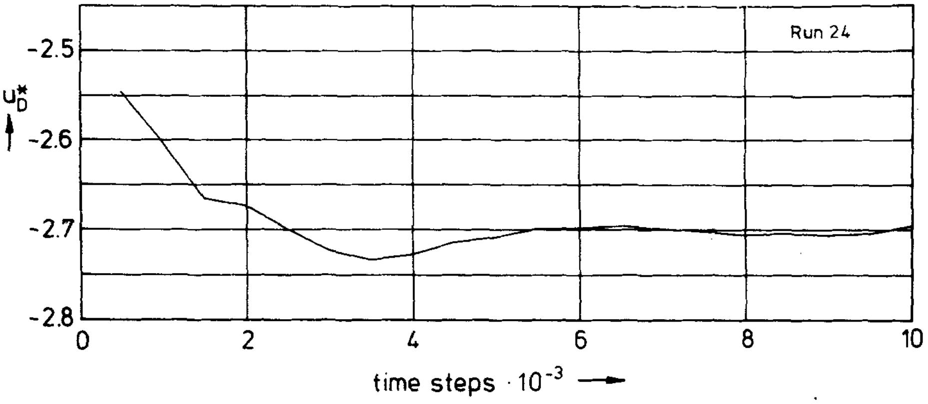

Figure 5b Running average of the dipolar energy contribution at $\rho^* = 0.142$, $T^* = 6.156$ and $\mu^{*2} = 12$ (run 24). This is an example for the gas.

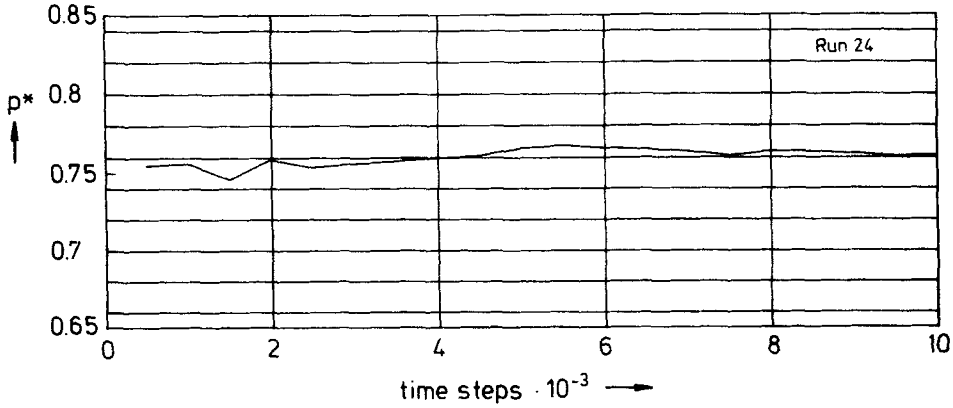

Figure 5c Running average of the total pressure at $\rho^* = 0.142$, $T^* = 6.156$ and $\mu^{*2} = 12$ (run 24). This is an example for the gas.

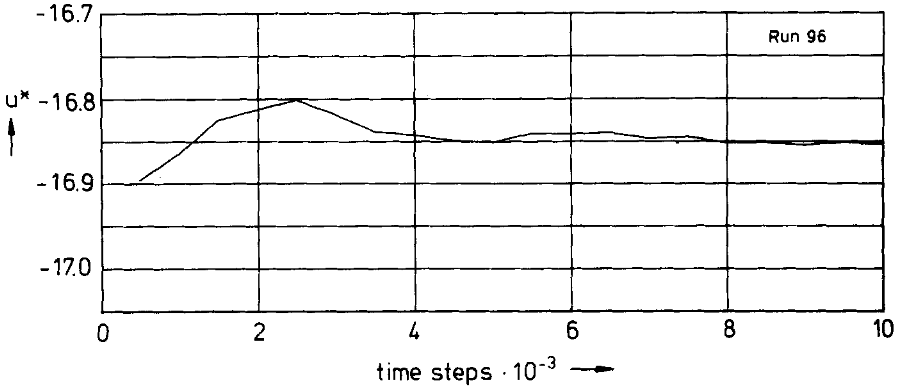

Figure 6a Running average of the configurational internal energy at $\rho^* = 0.54756$, $T^* = 6.156$ and $\mu^{*2} = 12$ (run 96). This is an example for the liquid.

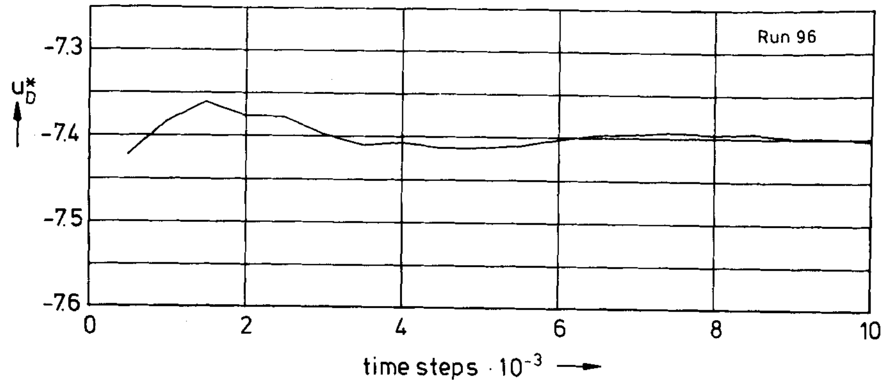

Figure 6b Running average of the dipolar energy contribution at $\rho^* = 0.54756$, $T^* = 6.156$ and $\mu^{*2} = 12$ (run 96). This is an example for the liquid.

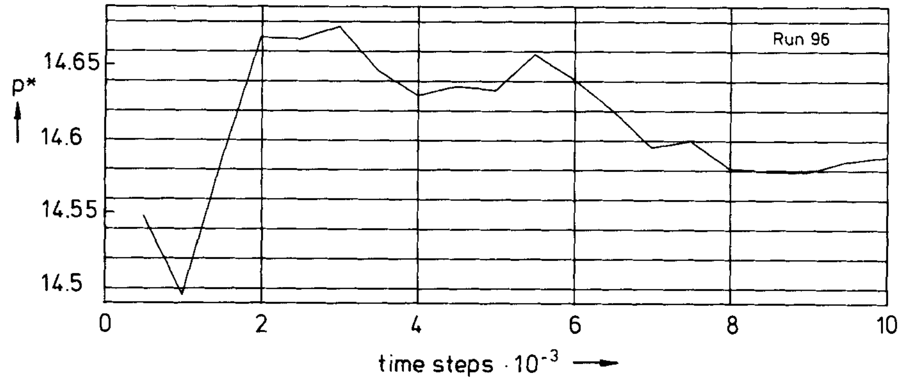

Figure 6c Running average of the total pressure at $\rho^* = 0.54756$, $T^* = 6.156$ and $\mu^{*2} = 12$ (run 96). This is an example for the liquid.

punkt programm "Thermophysikalische Eigenschaften neuer Arbeitsmedien der Energie- und Verfahrenstechnik", AZ.: Fi 287/5, gefördert. Einer der Autosen (S.F.) erinnert sich mit Dankbarkeit an die Einfuhrung in die Molekulasen Simulationen, die er von Henry Kehiaian bei der Faraday Discussion 1967 in Exeter erhielt.

APPENDIX A: IDEAL DIPOLE WITH RF

Forces

The force between two dipoles $\boldsymbol{\mu}_i$ and $\boldsymbol{\mu}_j$ is given by using $\mathbf{F}_D = -\nabla u_D$. This yields the force on dipole i

$$F_{D_{i,c}} = -\mu_{ia} \cdot T_{abc} \cdot \mu_{jb} \tag{A1}$$

where

$$T_{abc} = \nabla_a \nabla_b \nabla_c \frac{1}{r} \tag{A2}$$

or

$$T_{abc} = -\frac{15}{r^7} \cdot r_a \cdot r_b \cdot r_c + \frac{3}{r^5} \cdot (r_a \delta_{bc} + r_b \, \delta_{ac} + r_c \delta_{ab}) \cdot \tag{A3}$$

Because RF is not dependent on the distance vector $\mathbf{r}$, $T_{abc} = T_{\mathrm{RF}_{abc}}$ and thus RF does not contribute to the forces. Finally, the force vector is derived to be

$$\begin{aligned} \mathbf{F}_{D_i}(\mathbf{r}) = & \left[\frac{15}{r^7} (\boldsymbol{\mu}_i \cdot \mathbf{r}) (\boldsymbol{\mu}_j \cdot \mathbf{r}) - \frac{3}{r^5} \cdot \boldsymbol{\mu}_i \cdot \boldsymbol{\mu}_j \right] \cdot \mathbf{r} \\ & - \frac{3}{r^5} [(\boldsymbol{\mu}_i \cdot \mathbf{r}) \, \boldsymbol{\mu}_j + (\boldsymbol{\mu}_j \cdot \mathbf{r}) \, \boldsymbol{\mu}_i]. \end{aligned} \tag{A4}$$

Equation (A4) can be interpretated that the force consists of two vectors, one in $\mathbf{r}$-direction and the other laying in the $\boldsymbol{\mu}_i$, $\boldsymbol{\mu}_j$-plane.

Torques

The torque of an electrostatic field $\mathbf{E}$ acting on a dipole $\boldsymbol{\mu}_i$ is given by the cross-product

$$\mathbf{N}_{D_i} = \boldsymbol{\mu}_i \times \mathbf{E}(\mathbf{r}_i). \tag{A5}$$

With RF, the electrostatic field of dipole $\boldsymbol{\mu}_j$ acting on $\boldsymbol{\mu}_i$ is

$$\mathbf{E}_j(\mathbf{r}_i) = \mathbf{T}_{\mathrm{RF}}(\mathbf{r}) \cdot \boldsymbol{\mu}_j, \quad i \neq j\,. \tag{A6}$$

Thus the torque of dipole $\boldsymbol{\mu}_j$ on dipole $\boldsymbol{\mu}_i$ is

$$\mathbf{N}_{D_i} = \boldsymbol{\mu}_i \times \mathbf{E}_j(\mathbf{r}_i). \tag{A7}$$

From equation (A6) it becomes clear that using the modified $\mathbf{T}_{\mathrm{RF}}$-tensor, RF contributes to the torques.

APPENDIX B: ENERGY SCALING

NVE$_X$

From keeping the total energy U_{tot} constant, we rescale the translational velocities v_i and the angular velocities ω_i by

$$v_i^{\mathrm{new}} = S_{\mathrm{NVE}} \cdot v_i^{\mathrm{old}} \qquad \text{(B1)}$$
$$\omega_i^{\mathrm{new}} = S_{\mathrm{NVE}} \cdot \omega_i^{\mathrm{old}}$$

where

$$S_{\mathrm{NVE}} = \left(\frac{U_{\mathrm{kin,NVE}}}{U_{\mathrm{kin}}^{\mathrm{old}}}\right)^{1/2}. \qquad \text{(B2)}$$

The actual kinetic energy before scaling $U_{\mathrm{kin}}^{\mathrm{old}}$ and the kinetic energy for keeping total energy constant $U_{\mathrm{kin,NVE}}$ are given by

$$U_{\mathrm{kin}}^{\mathrm{old}} = \frac{1}{2} m \sum_i v_i^{\mathrm{old}^2} + \frac{1}{2} \mathrm{I} \sum_i \omega_i^{\mathrm{old}^2} \qquad \text{(B3)}$$

and

$$U_{\mathrm{kin,NVE}} = U_{\mathrm{tot}} - U_{\mathrm{2CLJD}}. \qquad \text{(B4)}$$

In equation (B4) U_{2CLJD} is the actual potential energy.

NVT$_X$

Temperature is kept constant by isokinetic scaling of the translational velocities and the angular velocities according to equipartition law:

$$v_i^{\mathrm{new}} = S_{\mathrm{tr}} \cdot v_i^{\mathrm{old}} \qquad \text{(B5)}$$
$$\omega_i^{\mathrm{new}} = S_{\mathrm{rot}} \cdot \omega_i^{\mathrm{old}}.$$

The scaling factors are given by

$$S_{\mathrm{tr}} = \left(\frac{[\sum_i v_i^2]_{\mathrm{NVT}}}{\sum_i v_i^{\mathrm{old}^2}}\right)^{1/2} \qquad \text{(B6)}$$

and

$$S_{\mathrm{rot}} = \left(\frac{[\sum_i \omega_i^2]_{\mathrm{NVT}}}{\sum_i \omega_i^{\mathrm{old}^2}}\right)^{1/2} \qquad \text{(B7)}$$

where

$$[\sum_i v_i^2]_{\mathrm{NVT}} = \frac{3NkT}{m} \qquad \text{(B8)}$$

and

$$[\sum_i \omega_i^2]_{\mathrm{NVT}} = \frac{2NkT}{\mathrm{I}} \qquad \text{(B9)}$$

are determined by the equipartition law for diatomics.

References

[1] M. Lupkowski and P.A. Monson, "Phase diagrams of interaction site fluids. II. Dipolar diatomics", *Molec. Phys.*,**67**, 53, (1989).

[2] C. Vega, B. Saager and J. Fischer, "Molecular dynamics studies for the new refrigerant R152a with simple model potentials", *Molec. Phys.*, **68**, 1079, (1989).

[3] B. Saager and J. Fischer, unpublished results (to be submitted to Fluid Phase Equilibria).

[4] V.M. Jansoone, "Dielectric properties of a model fluid with the Monte Carlo method", *Chem. Phys.*, **3**, 78, (1974).

[5] D.J. Adams and I.R. McDonald, "Thermodynamic and dielectric properties of polar lattices", *Molec. Phys.*, **32**, 931, (1976).

[6] S.W. de Leeuw, J.W. Perram and E.R. Smith, "Simulation of electrostatic systems in periodic boundary conditions. I. Lattice sums and dielectric constants", *Proc. R. Soc. A*, **383**, 27, (1980).

[7] P.P. Ewald, "Die Berechnung optischer und elektrostatischer Gitterpotentiale", *Ann.d.Phys.*, **64**, 253, (1921).

[8] H. Kornfeld, "Die Berechnung elektrostatischer Potentiale und der Energie von Dipol-und Quadrupolgittern", *Z. Phys.*, **22**, 27, (1924).

[9] A.J.C. Ladd, "Monte-Carlo simulations of water", *Molec. Phys.*, **33**, 1039 (1977).

[10] A.J.C. Ladd, "Long-range dipolar interactions in computer simulations of polar liquids", *Molec. Phys.*, **36**, 463, (1978).

[11] M. Neumann, "Dielectric properties and the convergence of multipolar lattice sums", *Molec. Phys.*, **60**, 225, (1987).

[12] J.A. Barker and R.O. Watts, "Monte Carlo studies of the dielectric properties of water-like models", *Molec. Phys.*, **26**, 789, (1973).

[13] L. Onsager, "Electric moments of molecules in liquids", J. Am. Chem. Soc., **58**, 1486 (1936).

[14] R. Lustig, "Angle-average for the powers of the distance between two separated vectors", *Molec. Phys.*, **65**, 175, (1988).

[15] S.W. de Leeuw, J.W. Perram and E.R. Smith, "Computer simulation of the static dielectric constant of systems with permanent electric dipoles", *Ann.Rev.Phys.Chem.*, **37**, 245, (1986).

[16] J.M. Haile, private communication (1985).

[17] C.W. Gear, "Numerical initial value problems in ordinary differential equations", Prentice Hall, Englewood Cliffs (1971).

[18] D.J. Evans, "On the representation of orientation space", *Molec. Phys.*, **34**, 317 (1977).

[19] D.J. Evans and S. Murad, "Singularity free algorithm for molecular dynamics simulations of rigid polyatomics", *Molec. Phys.*, **34**, 327, (1977).

[20] R. Lustig, A. Torro-Labbé and W.A. Steele, "A molecular dynamics study of the thermodynamics of liquid ethane", *Fluid Phase Equilibria*, **48**, 1, (1989).

[21] G. Ciccotti, M. Ferrario and J.-P. Rychaert, "Molecular dynamics of rigid systems in cartesian coordinates: A general formulation", *Molec. Phys.*, **47**, 1253, (1982).

[22] T.H. Jordan, H.W. Smith, W.E. Streib and W.N. Lipscomb, "Single-cristal x-ray diffraction studies of α-N_2 and β-N_2", *J.Chem. Phys.*, **41**, 756, (1964).

[23] D.J. Adams, E.M. Adams and G.J. Hills, "The computer simulation of polar liquids", *Molec. Phys.*, **38**, 387, (1979).

[24] M. Neumann, "Dipole moment fluctuation formulas in computer simulations of polar systems", *Molec.Phys.*, **50**, 841, (1983).

[25] J. Yao, R.A. Greenkorn and K.C. Chao, "Thermodynamic properties of Stockmayer molecules by Monte Carlo simulation", *J.Chem. Phys.*, **76**, 4657, (1982).

[26] D.J. Adams and E.M. Adams, "Static dielectric properties of the Stockmayer fluid from computer simulation", *Molec.Phys.*, **42**, 907, (1981).

[27] H.G. Petersen and S.W. de Leeuw, "Applied field simulations of Stockmayer fluids", *Molec.Phys.*, **66**, 637, (1989).

[28] H.J.M. Hanley and R.O. Watts, "Molecular dynamics calculation of the thermodynamic properties of methane", *Australian J. Phys.*, **28**, 315, (1975).

[29] J.L. Lebowitz, J.K. Percus and L. Verlet, "Ensemble dependence of fluctuations with application to machine computations", *Phys. Rev.*,**153**, 250, (1967).

[30] A. Torro-Labbé, R. Lustig and W.A. Steele, "Specific heats for simple molecular fluids from molecular dynamics simulations", *Molec. Phys.*, **67**, 1385, (1989).

[31] S.W. de Leeuw and N. Quirke, "Dielectric behaviour and multibody orientational correlations of dipolar molecular liquids", *J.Chem. Phys.*, **81**, 880, (1984).

[32] J. Fischer, R. Lustig, H. Breitenfelder-Manske and W. Lemming, "Influence of intermolecular potential parameters on orthobaric properties of fluids consisting of spherical and linear molecules", *Molec. Phys.*, **52,** 485, (1984).

[33] M. Bohn, B. Saager, K. Holzapfel and J. Fischer, "Studies on phase equilibria of two-centre Lennard-Jones fluids", *Molec. Phys.*, **59,** 433, (1986).

[34] D.B. McGuigan, M. Lupkowski, D.M. Paquet and P.A. Monson, "Phase diagrams of interaction site fluids. I. Homonuclear 12-6 diatomics", *Molec. Phys.*, **67,** 33, (1989).

[35] M. Bohn, J. Fischer and J.M. Haile, "Effect of molecular elongation on the quadrupolar free energy in diatomic fluids", *Molec. Phys.*, **65,** 797, (1988).

[36] M. Neumann, O. Steinhauser and G.S. Pawley, "Consistent calculation of the static and frequency-dependent dielectric constant in computer simulations", *Molec. Phys.*, **52,** 97, (1984).